ANALYSIS
https://doi.org/10.1038/s41893-019-0453-5

nature sustainability

There are amendments to this paper

The downstream air pollution impacts of the transition from coal to natural gas in the United States

Jennifer A. Burney

The recent shift in the United States from coal to natural gas as a primary feedstock for the production of electric power has reduced the intensity of sectoral carbon dioxide emissions, but—due to gaps in monitoring—its downstream pollution-related effects have been less well understood. Here, I analyse old units that have been taken offline and new units that have come online to empirically link technology switches to observed aerosol and ozone changes and subsequent impacts on human health, crop yields and regional climate. Between 2005 and 2016 in the continental United States, decommissioning of a coal-fired unit was associated with reduced nearby pollution concentrations and subsequent reductions in mortality and increases in crop yield. In total during this period, the shutdown of coal-fired units saved an estimated 22,563 (5%–95% confidence intervals (CI), 1,697–43,429) lives and 329 million (169–490 million) bushels of corn in their immediate vicinities; these crop estimates increase when pollution transport-related spillovers are included. Changes in primary and secondary aerosol burdens also altered regional atmospheric reflectivity, raising the average top of atmosphere instantaneous radiative forcing by 0.50 W m^{-2}. Although there are considerable benefits of decommissioning older coal-fired units, the newer natural gas and coal-fired units that have supplanted them are not entirely benign.

Over the past decade, the United States has increasingly relied on combustion of natural gas for the generation of electric power[1] (Fig. 1a–c). This shift in feedstock away from coal—driven in part by the rapid expansion of hydraulic fracturing and subsequent reductions in the price of natural gas—has generally been welcomed from a climate perspective. Natural-gas-fired units tend to release less CO_2 into the atmosphere on a per-energy basis[2,3], which has led to a substantial increase in sectoral CO_2 emissions efficiency[4] (Fig. 1c,d).

In addition to CO_2, however, the combustion processes that underlie electric power production also produce short-lived climate pollutants (SLCPs). Importantly, these co-emissions differ by feedstock and include various precursors of aerosol particulate matter (including respirable particulate matter with an aerodynamic diameter of less than 2.5 µm, $PM_{2.5}$) and ozone (O_3), as well as other harmful substances like carbon monoxide, heavy metals, benzene and other volatile organic compounds, and oxides of sulfur and nitrogen. Although CO_2 is long-lived and well-mixed in the atmosphere, and its impacts are therefore independent of where it is emitted, the same is not true for SLCPs. SLCPs typically remain closer to their emissions sources, evolve and interact physically and chemically in the atmosphere, and are known to contribute to a number of local- and regional-scale impacts, including damages to both human health and crop yields[5–7]. SLCPs also alter the radiative properties of the atmosphere, leading to changes in the atmospheric column temperature profile and surface energy balance that contribute to regional climate changes[8,9].

To understand the downstream impacts of a feedstock change, we would ideally monitor the full portfolio of emissions from each electric power generation unit, as well as a detailed suite of pollutant concentrations in the surrounding areas. This would enable us to track emitted compounds both chemically (as they evolve) and geographically (as they disperse). Through understanding how and where regional exposures change downstream from electric power plants, we could precisely measure whether and to what extent stack emissions of SLCPs affect people, plants and regional climate.

To date, this effort has been limited by gaps in both emissions data and concentration data. Only a subset of primary emissions are measured at power plant stacks: required continuous emissions monitoring systems (CEMS) report three gaseous species—CO_2, SO_2 and oxides of nitrogen (NO_x; Fig. 1d)—but do not report primary particulate matter, such as black carbon, organic carbon or fly ash (for reports such as the National Emissions Inventory, these quantities are instead estimated using emissions factors)[10,11]. Many of these primary emissions evolve and contribute to the formation of secondary pollutants and, although some of these secondary pollutants are monitored by the ground-based measurement networks maintained by the Environmental Protection Agency[12], coverage is only partial (chemically) and sparse (geographically). As a result, we cannot fully connect primary emissions to their final pollutant forms. Crucially, from a policy perspective, we are unable to determine how much of measured ambient $PM_{2.5}$ and other pollutants such as O_3 is attributable to power plants without inversion modelling (Supplementary Fig. 1) and, therefore, do not know the full costs of power plant emissions to weigh against their benefits.

This data gap is reflected in two bodies of literature that are focused on the impacts of SLCPs. Numerous empirical studies have established the statistical connection between exposure to secondary concentrations of $PM_{2.5}$ and O_3 and impacts on mortality and crop yields[13–18], but these studies cannot attribute changes in measured exposures to upstream technologies, actions or policies. A complementary body of literature uses climate and atmospheric chemical transport models (CTMs) to estimate changes in ambient pollutant concentrations that would evolve from a specified emission scenario, and then links those modelled environmental conditions to exposure–response functions to calculate impacts[19–24].

School of Global Policy and Strategy, University of California, San Diego, La Jolla, CA, USA. e-mail: jburney@ucsd.edu

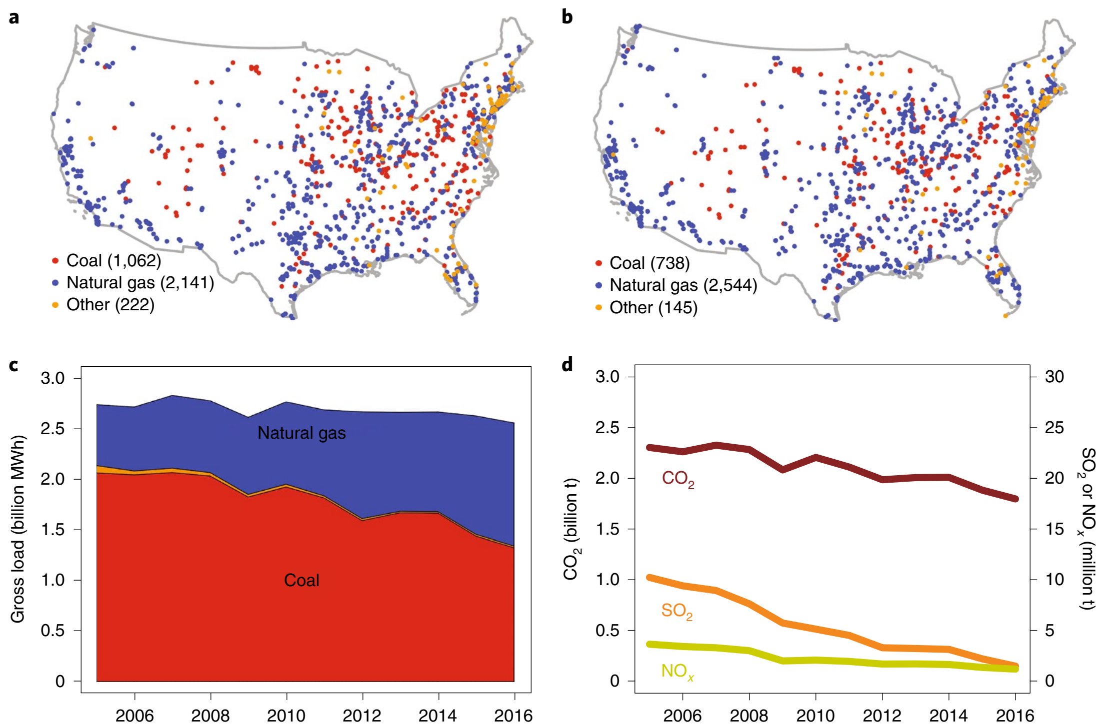

Fig. 1 | Locations of AMPD reporting fossil-fuel-burning electric power plants in the United States, by primary feedstock. a,**b**, Locations of AMPD reporting fossil-fuel-burning electric power plants in the United States at the start of 2005 (**a**) and at the end of 2016 (**b**). Details of timing are provided in Extended Data Fig. 1. **c**, The total share of natural gas as feedstock has increased, while total electric power production has remained fairly steady. **d**, Total emissions of CO_2, SO_2 and oxides of nitrogen (NO_x) from electric power generation have declined[1].

These integrated-assessment-type studies are more conducive to addressing policy questions, as CTMs can be used to model different regulatory environments and emissions scenarios[25–30], but they remain limited by the accuracy of the emissions inventories and exposure–response functions used[23].

The transition to natural gas in the United States provides a unique opportunity to bridge these two approaches with a large-scale natural experiment. The shift to natural gas has consisted mainly of the retirement of old coal-fired units and construction of new gas-fired units, resulting in the geographical redistribution of approximately 20% of US power generation infrastructure (Fig. 1, Extended Data Fig. 1). The decommissioning of old units and commissioning of new units represent discrete, location-specific changes in SLCP-emission fluxes into the surrounding environment that can be directly statistically linked to changes in ambient aerosol and O_3 concentrations, as well as to total pollution-related impacts on mortality, crop yields and regional radiative forcing (RF). This type of analysis has been used to estimate health impacts in other contexts, such as toxic releases[31] or desulfurization[32], and in detailed studies around individual coal plants[33] or smaller groups of plants[34–36]. The unique contribution of this study is its scope and its joint consideration of health, agriculture and regional climate impacts due to the change in pollution burden (aerosols, O_3 and other compounds) that have accompanied this large-scale energy transition.

Here I combined information on nearly all of the electric power generation units in the continental United States with validated satellite-based measurements of surface $PM_{2.5}$ and other pollutants, surface monitoring data, county mortality and crop yield data, and satellite observations of atmospheric aerosols and their properties. I estimated the average change in a set of pollution-related outcomes within each location, before and after an electric power generation unit was turned off or on, and controlling for both location-specific but time-invariant factors (such as different baseline levels of wealth across locations) and time-variant but location-independent factors (such as the national financial crisis) that might otherwise confound estimates of these relationships. As a robustness test, I also used an instrumental variables approach to further ensure that the statistical association between an outcome and the decommissioning or commissioning of a unit is isolated from other relevant factors that might be changing at the same place and time (see Methods). I then aggregated these multiple impact pathways to national-scale impacts on human mortality, crop production and regional radiative forcing (RF).

Results

Between 2005 and 2016, 334 coal-fired units at 138 facilities were taken offline and 612 new natural-gas-fired units came online across 243 facilities in the continental United States (Fig. 1a,b, Extended Data Fig. 1). A small fraction of these were direct upgrades (such as a new gas-fired unit replacing an older one), but the majority represented new capacity—either new units added to existing facilities, or new facilities entirely. As a result, although these changes (combined with advances in emissions controls technologies) produced net reductions in SO_2 and NO_x of more than 80% and 60%, respectively (Fig. 1d), local average fluxes of CO_2 and the co-emitted SLCPs into the ambient environment changed at hundreds of locations around the country, in both directions (Extended Data Fig. 1, Supplementary Fig. 2). Decommissioning of an older unit was associated with a ramping down of emissions during the previous year, whereas commissioning of a new unit was associated with a discrete increase in emissions followed by settling into a steady-state (Extended Data Fig. 2).

Although these units vary in size, technology and emissions controls, on average the decommissioning of a coal-fired unit was associated with a discrete and lasting reduction in steady-state surface aerosol $PM_{2.5}$ concentrations in the surrounding region (Fig. 2a), as measured by a combination of surface monitors and satellites (the data used are provided in Extended Data Fig. 3 and Supplementary Fig. 3).

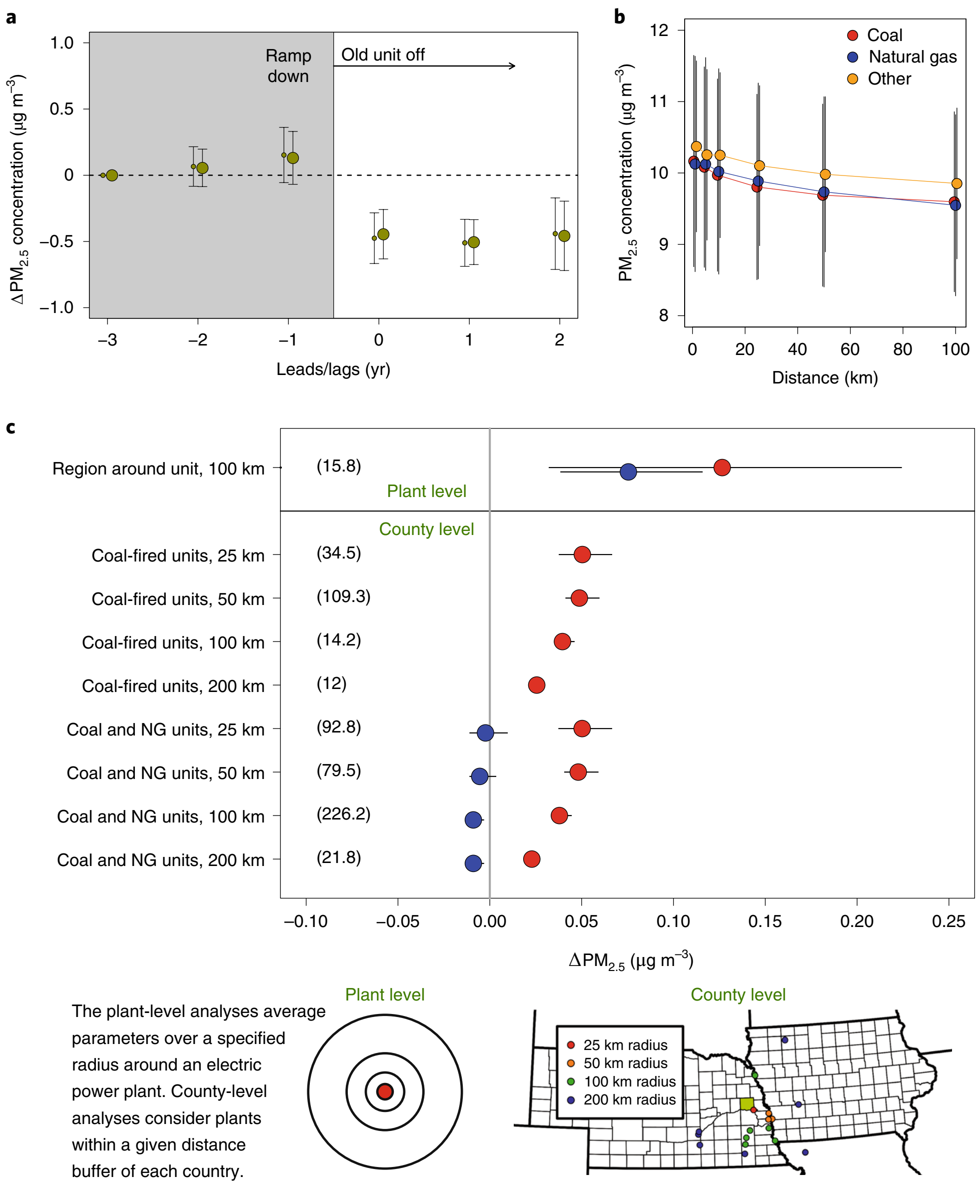

Fig. 2 | The impacts of old and new coal- and natural-gas-fired units on ambient $PM_{2.5}$ concentrations, as measured by a combination of satellite- and ground-based measurements. Impacts were measured using two methods, as indicated at the bottom of the figure. First, using the plant location as the unit of analysis and measuring changes around that location as a unit is turned off or on; and second, by aggregating to the county level and including the influence of new and old units within a specified distance buffer. **a**, The shutdown of coal-fired units is associated with an average unadjusted reduction of 0.5 μg m^{-3} in $PM_{2.5}$. **b**, Although this marginal change holds over large distances (small points, 5 km radius; large points, 100 km radius around units), the average $PM_{2.5}$ levels around operating power units decrease fairly rapidly with distance. **c**, Adjusting for temporal dynamics reduces the marginal effect of a shutdown by roughly half, and normalizing by average number of units shutdown at the same time (1.8) brings the estimate to 0.13 μg m^{-3} (top). At the county level, each coal-fired unit within 25 km is associated with an average county-level change of 0.05 μg m^{-3}, with smaller impacts for plants further away (bottom). NG, natural-gas-fired units. The values in parentheses show the *F*-statistics of the projected models, indicating that, even including controls for location- and time-specific confounding factors, the decommissioning of a coal-fired unit has a strong local pollution impact. Interestingly, natural-gas-fired units have a smaller and more localized impact on local $PM_{2.5}$. Estimates in **a** include location-level fixed effects, and estimates in **c** additionally include year fixed effects. The error bars show the 5%–95% CIs on the basis of s.e. clustered at the location (**a**) or county (**c**) level[1,65].

This marginal impact holds to more than 100 km, although average $PM_{2.5}$ concentrations are higher closer to operating units and decrease with distance (Fig. 2b). Accounting for location- and time-invariant effects lowers this effect to 0.23 μg m^{-3}, and normalizing for the average number of units shutdown at a given location and time (1.8) gives a per-unit estimate of 0.13 μg m^{-3} (Fig. 2c, top). Although the sign and significance of the impacts is robust, aggregating to the county level and allowing for different overall impact distances results in impact estimates that range between around 0.025 and 0.05 μg m^{-3} per unit shutdown (Fig. 2c, bottom; Supplementary Tables 1–3). Decommissioning of coal-fired units was also associated with reductions in observed tropospheric O_3, NO_2 and SO_2 (Supplementary Tables 4–6, Extended Data Fig. 4). NO_2 and SO_2 levels decrease with distance from an operating unit, but O_3 dynamics are more complicated (Supplementary Fig. 9). New natural-gas-fired units are also associated with higher ambient $PM_{2.5}$ levels at very local scales (Fig. 2c, Supplementary Table 3), as well as increased O_3 levels at the county level (Supplementary Table 4),

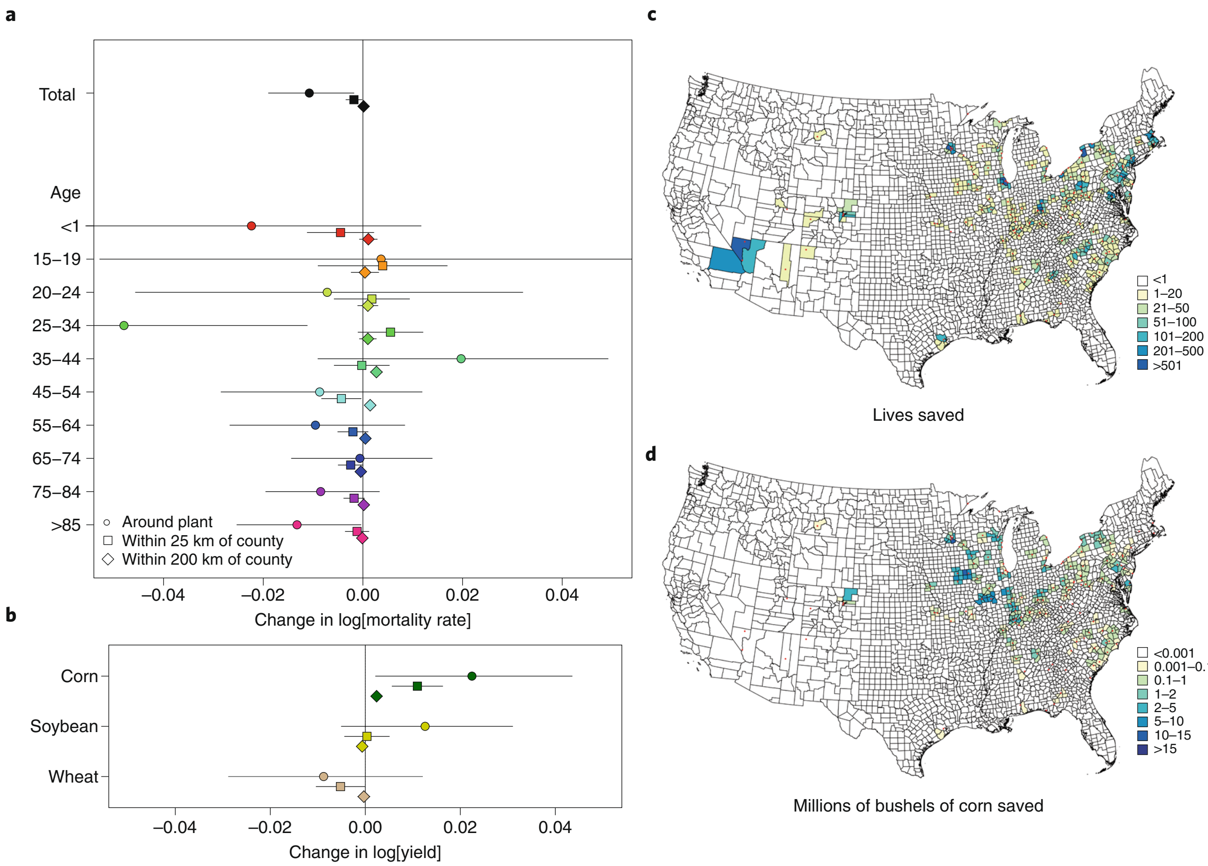

Fig. 3 | Changes in mortality rates and crop yields at the location and county level. a–d, Mortality rate (**a**) and crop yield (**b**) impacts associated with the decommissioning of coal-fired power units, and the geographical distributions of lives (**c**) and crops (**d**) saved. **a**,**b**, Estimates are shown for three models on the basis of their predictive power for pollution changes shown in Fig. 2. The plant location was used as the unit of analysis and each plant was matched to its county crop and demographic data (circles in **a** and **b**; this is the total effect of shutdowns and is not normalized by the average number of units closed simultaneously). Information was aggregated about all of the plants within a 25 km (squares in **a** and **b**) and 200 km (diamonds in **a** and **b**) radius to the county level to match with county data. Using the more local 25 km estimate at the county level (squares in **a** and **b**), the decommissioning of each coal-fired unit is associated with a 0.18% reduction (0.01–0.35%) in overall mortality rate. When broken down by age group, these effects more strongly impact the 45–84 age groups. Coal-unit shutdowns are also associated with an increase in corn yields of 1.1% (0.56–1.63%). All of the analyses include unit and year fixed effects to time-invariant location-specific factors as well as overall temporal shocks that might confound the relationship. The error bars show the 5%–95% CI on the basis of s.e. clusteredat the location or county level. The distribution of these impacts (central estimate) is shown in **c** and **d** for 25 km; crop impacts are statistically significant out to 200 km although mortality effects are not (200 km crop estimates are shown in Extended Data Fig. 9). Aggregating the more restricted local 25 km estimates suggests that the shift in feedstock away from coal saved 22,563 (16,896–43,428) lives and 329 million (169–490 million) bushels of corn production. Aggregating the 200 km crop impacts raises the central estimates to 1.8 billion bushels saved by decommissioningof coal-fired units between 2005 and 2016[1,37,74].

but the effects on O_3 of shutting down coal units and starting up natural-gas units are more difficult to disentangle due to the larger spatial scales and nonlinearities in O_3 formation (Extended Data Figs. 4 and 5). An individual example of the aggregate results that are reported in Fig. 2 is provided in Extended Data Fig. 6, and these impacts are also estimated on a per-MWh basis in Supplementary Tables 3–6.

These lower aerosol and O_3 concentrations conferred near-immediate benefits to health and crop productivity. Matching plants to counties using two methods (see Methods) revealed that counties with a coal-fired-unit shutdown in their immediate vicinity (Fig. 2, Supplementary Fig. 4) experienced an average associated 0.18% (0.01–0.35%) reduction in total all-cause mortality rate following each unit decommissioning, which was concentrated in older age groups (Fig. 3a). These counties also benefited from increases in corn yields of 1.1% (0.56–1.63%). Importantly, these estimates represent total impacts across all pathways for $PM_{2.5}$ and other covarying pollutants—the impacts of aerosol on mortality are largely via circulatory and respiratory pathways, but the estimates provided here also include lesser pathways and impacts of O_3 and other stack-related co-emissions. Similarly, crop impacts are due to the total combination of aerosol effects on radiation, temperature and precipitation, as well as potential direct deposition impacts, combined with O_3 and O_3 precursor-related plant damage. Results from instrumental variables estimates (see Methods), which should represent the portion of outcomes that are only attributable to the pollution-related impacts of a unit shutdown (or startup), are highly consistent with the reduced-form estimates (but with expected larger error bounds; Extended Data Fig. 7, Supplementary Table 2), providing strong evidence that the direct relationship observed between unit shutdown and human outcomes is robust. Despite their association with higher local $PM_{2.5}$ and county-scale O_3 levels, new natural-gas- and coal-fired units that come online during the time period were not robustly associated with increased all-cause mortality or decreased crop yields during the period of study (Supplementary Table 2, Extended Data Fig. 8).

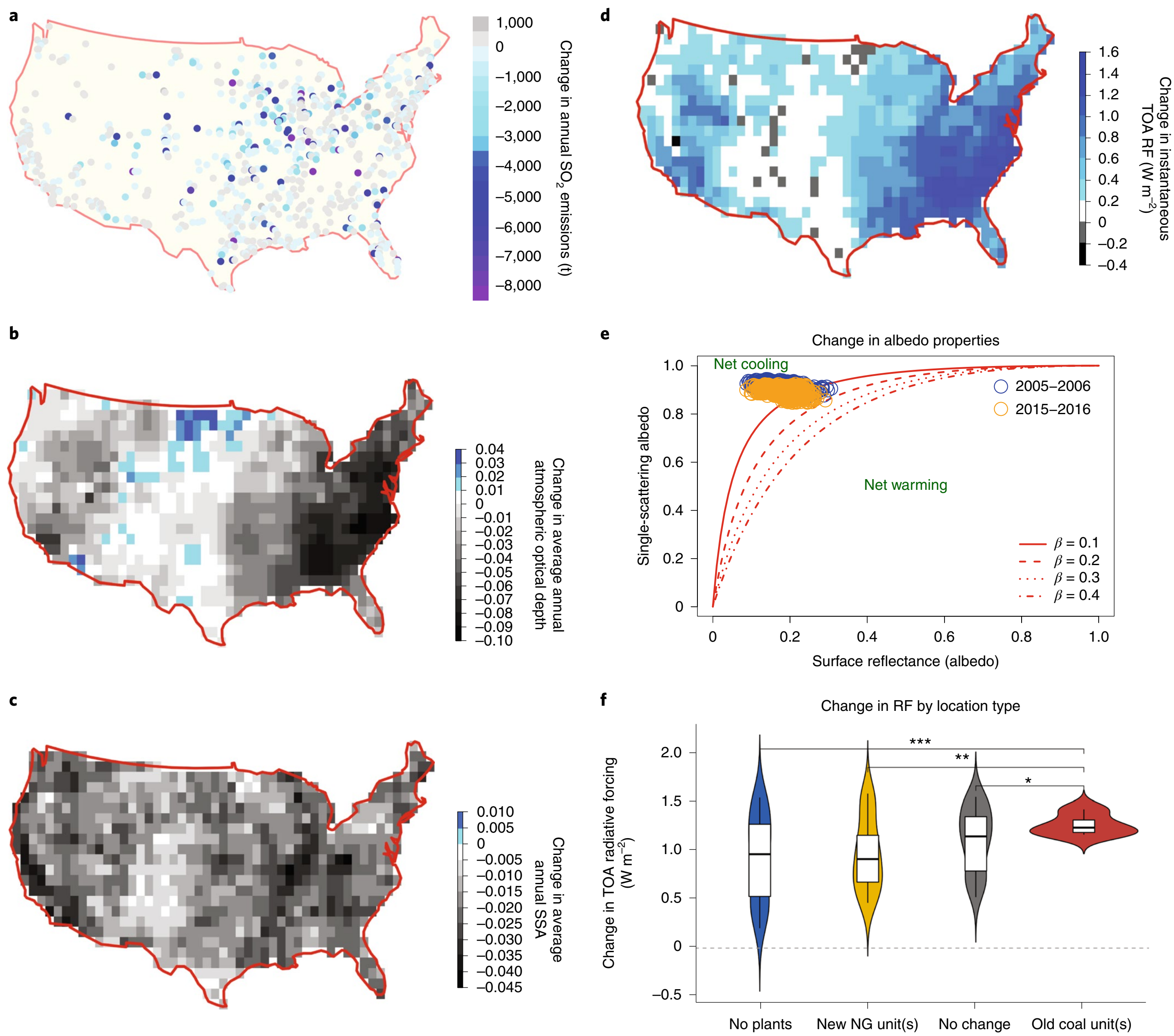

Fig. 4 | Regional RF changes due to electric power sector changes, 2005–2016. a, Change in annual SO_2 emissions at all of the fossil-fuel-based power plants in the United States throughout the analysis period. **b**,**c**, The corresponding changes in atmospheric optical depth data from the Moderate Resolution Imaging Spectroradiometer (MODIS; **b**) and SSA data from the Ozone Monitoring Instrument (OMI; **c**); the atmosphere became both cleaner and less optically reflective. **d**, The decreased reflectivity of the atmosphere translated into an increase in TOA clear sky RF across most of the country. **e**, Although the net effect of the aerosol mix remained cooling, the reduction of the so-called sulfate mask nudged the region towards net aerosol warming of the surface. Each 1° grid cell is plotted as a circle, at the beginning and end of the time period. **f**, Changes in RF are strongly and significantly different by location, and grid cells with decommissioned coal-fired units showed the strongest RF changes[1,70–73]. *P < 0.1; **P < 0.05; ***P < 0.01.

The pollution-related benefits of coal-unit shutdowns were heterogeneous across the continental United States. Figure 3c,d shows the distribution of mortality reductions and crop yield gains over the period of study. These impacts were calculated by multiplying the average effects (Fig. 3a,b) by the county's average mortality rate (or corn, wheat or soybean yield) and then scaling by population or cropped areas to obtain total impacts; a persistence of effects was assumed, as suggested by Fig. 2a. In total, the shutdown of coal-fired units saved an estimated 22,563 (16,896–43,428) lives and 329 million (169–490 million) bushels of corn production in the immediate vicinities of the coal-fired units during this time period. When pollution transport-related spillovers are included out to 200 km (Extended Data Fig. 9), these estimates increase to 1.8 billion (0.9–2.7 billion) bushels across the affected counties between 2005 and 2016. The inverse calculation of benefits foregone by not shutting a unit down suggests that coal-fired units remaining online caused 141,588 (10,647–272,528) deaths and the loss of 2.6 billion (4.4–15.8 billion) bushels of crops over the time period (these values are for the 25 km estimate; both this estimate and the higher 200 km estimate for corn are shown in Extended Data Fig. 9). For reference, this is roughly equivalent to a fifth of a recent year's production – the United States produced 14.4 billion bushels of corn in 2017[37].

The change in local emissions fluxes due to geographical shifts in the electric power generation fleet also had important impacts on regional RF. Changes in instantaneous top-of-the-atmosphere (TOA) RF due to aerosols are a function of shifts in both aerosol concentrations and composition (see Methods; Supplementary Information). The transition away from coal resulted in an 80% reduction in the power-plant-associated sulfur dioxide burden nationally (Fig. 1d); the geographical distribution of these reductions is shown in Fig. 4a. As described above, this emissions reduction not only translated into a reduction in the concentrations of overall surface particulate matter close to power plants, but also contributed to net $PM_{2.5}$ reductions at greater distances across the country (Extended Data Fig. 3) and related reductions in overall aerosol optical depth (AOD; Fig. 4b). The reduction in $PM_{2.5}$ associated with the decommissioning of coal-fired units comprised an unknown combination of black carbon, organic carbon, sulfate and nitrate aerosols, but atmospheric observations suggest that more of this reduction was in the form of scattering sulfates (formed from SO_2 and, to a lesser extent, NO_x) than absorbing black carbon—the single-scattering albedo (SSA) decreased over most of the region, indicating that the remaining aerosol mixture was more optically absorbing than at the beginning of the time period (Fig. 4c). These trends are statistically related—controlling for gross load, AOD reductions were greatest over areas with the largest reductions in SO_2 emissions ($P<0.1$), and SSA decreased most in locations with the largest combined reductions in load and SO_2 emissions ($P<0.05$).

The decreased reflectivity of the atmosphere translated into an increase in instantaneous TOA RF across most of the United States, with an average increase of $0.50\,W\,m^{-2}$ over the country, and of more than $1.5\,W\,m^{-2}$ in the southeastern part of the country (Fig. 4d, Supplementary Fig. 5). This is approximately equal in magnitude to the global average cooling that was estimated by the Intergovernmental Panel on Climate Change (IPCC) in the most recent 5th Assessment Report[38]. The relationship between changes in RF and changes in surface temperature is dependent on a number of factors, including the SSA of column aerosols, the surface albedo and the aerosol backscattering coefficient β (refs. [39–41]). Figure 4e shows the transition point between net warming and cooling effects at the surface for different values of β. Although the aerosol radiative effect remains net cooling over the country (assuming that $\beta \approx 0.13$), the distribution has moved towards net warming (see Methods). Figure 4f provides further evidence that these radiative changes are indeed due to the electric power sector transition—grid cell locations with decommissioned coal units showed the largest increases in RF and were statistically different from locations with other types of units and from locations with no units. An analysis of locations with no units and locations with units but no changes over the study period showed 95% CIs for total RF changes that overlap zero, as expected. The spatial overlap of both emissions (some new units are installed in locations with existing units, for example) and concentrations (the spatial scale is coarse and aerosols are transported outside the column into which they are emitted) likely explains why locations with new coal- and natural-gas-unit locations also show slight increases in RF.

Discussion

This analysis provides an integrated empirical assessment of pollution-related impacts that have accompanied the national-scale shift from coal to natural gas as a feedstock for electric power production. Although epidemiological exposure studies have documented various health and crops impacts of aerosols[15,42–45] and ozone[18,46–48], CTM-based studies have modelled the human and climate impacts of different emissions scenarios[22–24,49,50] and empirical studies have examined the impact of electric power generation emissions over smaller spatial scales[33–36], this study provides a nationwide empirical assessment of this sectoral shift in the United States.

The reduced-form estimates for mortality presented here are similar to previous large exposure studies, including a recent meta-analysis[51] (Extended Data Fig. 10). However, mortality estimates using unit shutdown as an instrument for $PM_{2.5}$ (and covarying pollutant) exposure changes are notably higher (a more detailed comparison of the results is provided in the Supplementary Information). The estimated national impacts are also higher than those estimated in a recent study into the mortality benefits of switching from coal to solar power[27]. This may be due to the fact that the estimates presented here capture the impacts of all covarying pollutants from a unit shutdown (and not just $PM_{2.5}$), and also because changing background levels of pollution (Extended Data Fig. 3) matter if overall exposure–response curves are nonlinear. These results underscore the need for more causally-identified observational studies to understand the impacts of technology changes and to improve modelling studies (in part by disentangling the impacts of individual pollutants that are captured together here). Recent research showed that, although CTMs perform well on average[21,22], model-based impact estimates are extremely sensitive to the exposure–response relationships used[23], and remain limited by both uncertainties in estimated emissions inventories and overall computational power and resolution. Perhaps most importantly, this analysis jointly considers agriculture and regional RF in addition to human health. The impacts of aerosols and O_3 on agriculture are relatively understudied in comparison with mortality; this analysis suggests—in line with previous studies[7,18,47,52]—that agricultural effects are sizable and would meaningfully impact any accounting of benefits and costs.

A full accounting of the costs and benefits of the transition to natural gas should include spatially resolved effects of both old and new units. Over the period of this study, on both a per-unit and per-kWh basis, newer natural-gas- and coal-fired units were not associated with broad negative downstream mortality and crop impacts (Supplementary Tables 2 and 7–9). However, these new units should not be assumed to be benign, as they are associated with some changes in ambient levels of $PM_{2.5}$, NO_2 and O_3 (Supplementary Tables 3–6). This highlights the need for more research in several areas. The particulate matter associated with natural-gas-fired units is probably comprised of secondary nitrate aerosols, as opposed to a combination of sulfate and carbonaceous aerosols from coal combustion[53]. Further research is needed to assess whether CTMs are reproducing this secondary aerosol formation correctly[54], and whether this different aerosol mix leads to similar health and agricultural impacts as coal $PM_{2.5}$. Research on the differential toxicity of $PM_{2.5}$ types suggests that these might vary by a factor of 5 (refs. [13,55–57]). Beyond health, we would expect that aerosol direct, indirect and semi-direct effects all change as a function of the composition of the particulate mix, with important impacts for crops and regional climate. This analysis therefore underscores the importance of investment in more comprehensive monitoring of emissions at the stack level and in ground-based networks (more speciated $PM_{2.5}$ sites) for assessing such impacts[58]. Consistent with previous research[59], this study shows that O_3 formation is nonlinear and less confined to the regions that surround units (Supplementary Figs. 8 and 9), and highlights the need for more research across spatial scales to better understand changes in O_3 downstream from large emissions flux changes across a range of background conditions.

Although the associated mortality and crop yield benefits are large for the coal-to-natural-gas transition, the transition is also responsible for reducing the size of the sulfate mask, which is presently offsetting CO_2-related warming. The cleaning of the air associated with this feedstock change has therefore raised regional instantaneous TOA RF; this analysis shows that the regional aerosol mix is shifting from net cooling to net warming. Further decommissioning of coal-fired units would be expected to contribute to increased instantaneous TOA RF; this could accelerate total local anthropogenic warming, although assessment of steady-state total RF impacts requires the inclusion of longer-run impacts from CO_2 emissions. Nevertheless, these empirical findings—in broad agreement with model-based estimates[21,60]—highlight the importance of educating both policymakers and citizens about the expected short-term climate consequences of cleaning the air.

This analysis has several important limitations. First, the impacts of coal-unit shutdowns in the future could differ from the results presented here, due to differences in feedstocks regionally, the evolution of technology over time and the fact that the oldest, least-efficient coal-fired units are probably retired first. Furthermore, socio-economic confounding factors may affect the external validity of these results in cases in which plant siting and shutdown decisions target (or exclude) vulnerable populations. Moreover, if upwind–downwind relationships between exposed populations and crops and power plants are not as-if random when aggregated annually, the effects measured here would be biased. This analysis only deals with a subset of SLCPs and their outcomes, but morbidity, decreased productivity and economic losses, and human-capital-related outcomes such as test scores and absenteeism have been shown to be related to $PM_{2.5}$ and other pollutant concentrations. Moreover this analysis does not address the impacts of unmeasured coemissions, many of which are known to have detrimental impacts on humans and/or plants. On the climate side, this analysis only addresses direct instantaneous clear-sky RF, and not steady-state RF. Power plant CO_2 and methane emissions also contribute to longer-run RF changes and, therefore, understanding the full steady-state response will require additional research. Furthermore, aerosols affect cloud formation and precipitation, potentially leading to a host of downstream impacts (Supplementary Information). Finally, this analysis is limited to combustion-related pollution effects and does not include upstream life-cycle emissions associated with feedstock extraction that may be substantial[61] and have a very different geographical distribution. Similarly, this analysis does not address important changes in emissions control technologies that have taken place in recent decades and have contributed to reduced SLCP emissions.

Policymakers often discuss greenhouse gas emissions and anthropogenic climate changes as distinct and separable from air pollution, but a growing number of studies emphasizes that the same combustion processes simultaneously produce both CO_2 and the SLCPs analysed here[62,63] (Supplementary Information). This analysis of pollution-related impacts provides a framework for more thoroughly and accurately assessing the costs and benefits of investments in energy infrastructure. Historically, policies and investments in mitigation of CO_2 emissions from the electric power sector have only weighed the cost of the technology change (immediate, large and locally borne) against globally shared and more uncertain future benefits from greenhouse gas reductions. As a result, the financial case for mitigation, especially with heavy discount rates, has been weak. This analysis suggests a much broader scope for cost–benefit analyses of CO_2 mitigation by including co-emitted SLCPs. The impacts of these co-emissions are local, fast-acting, large and cross-sectoral; they are also strongly heterogeneously distributed. Thus, spatially explicit accounting for the full suite of emissions associated with electric power production could potentially lead to much deeper optimal levels of mitigation and new cross-sectoral coalitions of beneficiaries[64].

Methods

Data sources. *Power plant data.* Power plant data were obtained from the US Environmental Protection Agency's (EPA) Air Markets Program Database (AMPD), which includes information on nearly all of the operating fossil-fuel-based power plant units in the United States, including location, primary and secondary fuels, total load, operating status and time, technology type, emissions controls types and continuous emissions monitoring systems (CEMS) measurements of CO_2, SO_2 and NO_x from each unit (by mass)[1]. I coded units with primary feedstock of any coal or petroleum coke as coal-fired units, primary feedstock of natural gas of any sort as natural-gas-fired units and primarily feedstock of diesel, oil, biomass or other wastes as 'other'. Units that were used intermittently were considered to be operational until fully shut down.

SLCP data. I used two main sources of surface-level air pollution data. The first is satellite-based surface $PM_{2.5}$ data from the atmospheric composition group at Dalhousie University[65]. These data were created by fitting a weighted ensemble of satellite-based AOD measurements to ground-based $PM_{2.5}$ measurements (EPA monitors in the United States), accounting for temperature, relative humidity and aerosol layer height. Data were then extrapolated spatially using these other factors in a geographically weighted regression. As shown in Supplementary Fig. 3, these data agree well with surface EPA monitor data, but show a smaller response, potentially due to measurement error (Extended Data Fig. 8); I therefore conducted analyses using both datasets. Surface data for $PM_{2.5}$ and O_3 were obtained from the US EPA monitor data collated for the agency's annual air quality reports[12,66]. The surface O_3 data do not agree as well with satellite column data (OMI)[67] and, therefore, filled surface data were used in these analyses at the expense of measurement error over extrapolated areas. I gridded the underlying data to 0.25° resolution and then filled the surface data using nearest neighbours (Supplementary Fig. 3).

Atmospheric column data. Atmospheric column data were obtained from the satellite-based OMI and MODIS instruments. OMI provides information on planetary boundary layer SO_2 (ref. [68]) and tropospheric column NO_2 (ref. [69]), as well as single scattering albedo (SSA) of column aerosols at 470 nm (ref. [70]), gridded to either 0.25° or 1.0°. MODIS provides AOD at 550 nm at 1° resolution[71]. For all of the satellite products, I aggregated level-2 gridded daily data products to annual averages. To calculate RF (Fig. 4d–f), I used cloud fraction data obtained from the Atmospheric Infrared Sounder (AIRS)[72]. To link RF to surface temperature (Fig. 4e), I used the Modern-Era Retrospective Re-Analysis (MERRA) land surface albedo data[73].

Human outcomes data. Data on mortality by county were obtained from the Centers for Disease Control (CDC) National Vital Statistics Service (NVSS) database[74], and crop yield data by county were obtained from the US Department of Agriculture (USDA) National Agricultural Statistics Service (NASS) database[37]. Human outcomes data were matched to data on power generation units using county and state names.

Empirical impact estimation. This analysis used a steady-state box model approach to assess the impacts of emissions from power plants on ambient surface pollution, human outcomes and atmospheric properties. I did this in two ways. First, I used the geographical location as the unit of analysis and, following an empirical logic used in previous environmental studies[31], I matched stack locations with ambient environmental conditions (such as $PM_{2.5}$ concentrations) and mortality and crop yield data from the county in which the unit is located. I treated the known technology or feedstock change within the grid cell as exogenous, and the relative timing of technology and feedstock changes between different locations as-if random. I then compared conditions and outcomes in a given location before and after a unit was turned on or off, by feedstock type, using panel regression analysis:

$$y_{it} = \alpha_i + \theta_t + \beta \mathbf{X}_{it} + \epsilon_{it} \quad (1)$$

Here y is the outcome of interest—either a proximate environmental outcome, such as ambient concentrations of a given pollutant or column aerosol properties, or a more downstream human outcome, such as crop yields or mortality. The analysis was conducted for a panel set of observations of grid cells i in the United States, for years t between 2005 and 2016. β is the main quantity of interest—the impact of a change in technology $\mathbf{X}$ on the outcome y. α_i are unit-level fixed effects, accounting for time-invariant location-specific characteristics that might affect y (such as differing average local climate across power plant locations), and θ_t are time fixed effects, accounting for universal phenomena occurring in specific years that might affect y (such as the global financial crisis). Inclusion of α_i and θ_t means that the analysis compares each location to itself before and after a unit is turned off or on, and the predicted value $\hat{\beta}$ is then the average effect across all of the locations of such a change.

In the most straightforward form, this switching off or on of a unit ($\mathbf{X}_{it}$) is coded as binary, and $\hat{\beta}$ therefore represents the average impact on y of a unit being turned off or on. However, because not all units are the same, I also conducted the analysis using a continuous measure of gross load for $\mathbf{X}_{it}$; in this framing, $\hat{\beta}$ is then the average effect across all of the locations associated with production of a given amount of electric power (Supplementary Tables 3–5, in millions of MWh). I conducted the analysis in both totals by unit and on a per-MWh basis, because human, crop and climate impacts are a function of total emissions, whereas cost–benefit analyses and comparisons between potential future counterfactual scenarios are often more appropriate on a per-energy-unit basis. It is important to note that estimates using operating load as a predictor variable are potentially more susceptible to confounding by factors (such as economic activity) that affect both electric power demand and outcomes of interest.

In addition to relating these technology changes to ambient conditions around power plants, I also assessed the impact on environmental parameters at increasing radii around the location of the power generation unit (Extended Data Fig. 4). For robustness, I estimated impacts using several universes of observational units, leads and lags models (Supplementary Tables 1–5), and an instrumental variables (IV) approach (Supplementary Table 2, Extended Data Figs. 7 and 8). The IV specification strips away the variation in $PM_{2.5}$ that is not associated with the decommissioning of a coal-fired power plant unit, and then relates that remaining variation in $PM_{2.5}$ to the final outcome of interest (such as mortality). All of the results include s.e. for $\hat{\beta}$, corrected for clustering at the unit/location, or unit/location and year, levels as noted in the figure and table captions. This accounts for the fact that repeated observations of the same location over time probably do not have an independent error structure.

Although estimating the impacts in the region surrounding an electric power plant makes sense for environmental parameters, it does not allow easy assessment of effects over larger spatial scales. I therefore also conducted impact analysis at the county level by aggregating information about all plants within (1) a 25 km radius and (2) a 200 km radius from the county centroid.

$$y_{ct} = \alpha_c + \theta_t + \sum_k \beta_k Nr_{kct} + \epsilon_{ct} \quad (2)$$

In this equation, c is the county and Nr_{kct} is the number of units of a given feedstock type k within radius r of the county. As this model also includes year and county fixed effects, all variation comes from the switching on and off of units and the analysis compares outcomes in a county before and after a unit is switched on or off within a specified distance band. Here I report both 25 km and 200 km results, as they span the sizes of the counties in the sample (Supplementary Fig. 4) and capture the scale over which measurable impacts persist (Figs. 2 and 3).

I aggregate totals to the continental United States (such as deaths and crop production; Fig. 3, Extended Data Fig. 9) by multiplying the estimated impact coefficient $\hat{\beta}$ by the number of units switched, baseline mortality and population (or yields and cropped areas) and the number of years of impact over the study period.

RF and the sulfate mask. Following a previous publication[39] as well as other studies[40,41,75,76], I calculated the instantaneous TOA RF as the change in downward minus upward radiation at the TOA, without any equilibration by the stratosphere:

$$\Delta F \approx -DS_0 T_{\mathrm{atm}}^2 (1-f_c)\omega\overline{\beta}\delta \times \left((1-R_s)^2 - \frac{2R_s}{\overline{\beta}}\left(\frac{1}{\omega} - 1\right)\right) \quad (3)$$

Here D is the daylight fraction (average of 0.5 for the year), S_0 is the solar constant—1,361 W m^{-2}—and T_{atm} is the transmissivity of the atmosphere. I used a T_{atm} value of 0.76 based on a previous study[39], as an average of literature values. I used a value of $\overline{\beta} = 0.13$ on the basis of a previous report[77]. For f_c, the cloud fraction, I used average values provided by AIRS over the time period 2005–2015 (data were not available for the entire year of 2016)[72]. Finally, for surface reflectance R_s, I used average data from the beginning (2005–2006) and end (2015–2016) of the analysis period from MERRA[73]. I calculated IRF for the beginning two years and final two years (average), and subtracted to estimate the change in IRF (Fig. 4, Supplementary Fig. 5).

The critical value C shown in Fig. 4e, whereby an aerosol layer is net cooling versus net warming, is defined as:

$$\omega < \frac{2R_s}{(\overline{\beta}(1-R_s)^2 + 2R_s)} \quad (4)$$

In Fig. 4e, I plotted all 1.0°×1.0° grid cells (circles) to show the distribution of SSA and surface albedo across the United States at the beginning and end of the analysis period. The assessment of whether the regional aerosol mix has net positive or negative radiative impacts depends on the backscattering ratio. Haywood and Shine[39] suggest larger values (for example, ≥0.21), whereas more recent comparisons, such as ref. [77], suggest smaller values of ~0.10–0.13. For values up to $\overline{\beta} = 0.2$, the distribution of IRF does move to a mix of net warming and cooling from the beginning of the analysis period, when it is all net cooling.

Data availability

All data used in these analyses are publicly available, as described above. Processed, compiled datasets to replicate these analyses are available at https://doi.org/10.7910/DVN/RIZQUN.

Code availability

Code to generate compiled data and to replicate all of the analyses here (results, figures, tables) is available at https://github.com/jaburney/naturalgastransition.

Received: 28 February 2019; Accepted: 11 November 2019;
Published online: 6 January 2020

References

1. *Air Markets Program Data* (EPA, accessed 13 April 2018); https://ampd.epa.gov/ampd/
2. Schrag, D. P. Is shale gas good for climate change? *Daedalus* **141**, 72–80 (2012).
3. Hughes, J. D. Energy: a reality check on the shale revolution. *Nature* **494**, 307–308 (2013).
4. de Gouw, J. A., Parrish, D. D., Frost, G. J. & Trainer, M. Reduced emissions of CO_2, NO_x, and SO_2 from U.S. power plants owing to switch from coal to natural gas with combined cycle technology. *Earth's Future* **2**, 75–82 (2014).
5. Rogelj, J. et al. Disentangling the effects of CO_2 and short-lived climate forcer mitigation. *Proc. Natl Acad. Sci. USA* **111**, 16325–16330 (2014).
6. *Integrated Assessment of Black Carbon and Tropospheric Ozone: Summary for Decision Makers* (UNEP and WMO, 2011).
7. Proctor, J., Hsiang, S., Burney, J., Burke, M. & Schlenker, W. Estimating global agricultural effects of geoengineering using volcanic eruptions. *Nature* **560**, 480–483 (2018).
8. Shindell, D. T., Faluvegi, G., Rotstayn, L. & Milly, G. Spatial patterns of radiative forcing and surface temperature response. *J. Geophys. Res. Atmos.* **120**, 5385–5403 (2015).
9. Persad, G. G. & Caldeira, K. Divergent global-scale temperature effects from identical aerosols emitted in different regions. *Nat. Commun.* **9**, 3289 (2018).
10. *2014 National Emissions Inventory Report* (EPA, 2014); https://gispub.epa.gov/neireport/2014/
11. *Clearinghouse for Inventories and Emissions Factors (CHIEF)* (EPA, 2018); https://www.epa.gov/chief
12. *Air Quality System (AQS)* (EPA, 2019); https://www.epa.gov/aqs
13. Bell, M. L., Ebisu, K., Peng, R. D., Samet, J. M. & Dominici, F. Hospital admissions and chemical composition of fine particle air pollution. *Am. J. Respir. Crit. Care Med.* **179**, 1115–1120 (2009).
14. Pope, C. A. III et al. Lung cancer, cardiopulmonary mortality, and long-term exposure to fine particulate air pollution. *JAMA* **287**, 1132–1141 (2002).
15. Thurston, G. D. et al. Ambient particulate matter air pollution exposure and mortality in the NIH-AARP diet and health cohort. *Environ. Health Perspect.* **124**, 484–490 (2015).
16. Long, S. P., Ainsworth, E. A., Leakey, A. D. & Morgan, P. B. Global food insecurity. Treatment of major food crops with elevated carbon dioxide or ozone under large-scale fully open-air conditions suggests recent models may have overestimated future yields. *Proc. R. Soc. B* **360**, 2011–2020 (2005).
17. Feng, Z. & Kobayashi, K. Assessing the impacts of current and future concentrations of surface ozone on crop yield with meta-analysis. *Atmos. Environ.* **43**, 1510–1519 (2009).
18. McGrath, J. M. et al. An analysis of ozone damage to historical maize and soybean yields in the United States. *Proc. Natl Acad. Sci. USA* **112**, 14390–14395 (2015).
19. Van Dingenen, R. et al. The global impact of ozone on agricultural crop yields under current and future air quality legislation. *Atmos. Environ.* **43**, 604–618 (2009).
20. Cohen, A. J. et al. Estimates and 25-year trends of the global burden of disease attributable to ambient air pollution: an analysis of data from the global burden of diseases study 2015. *Lancet* **389**, 1907–1918 (2017).
21. Shindell, D. et al. Simultaneously mitigating near-term climate change and improving human health and food security. *Science* **335**, 183–189 (2012).
22. Lelieveld, J., Evans, J. S., Fnais, M., Giannadaki, D. & Pozzer, A. The contribution of outdoor air pollution sources to premature mortality on a global scale. *Nature* **525**, 367–371 (2015).
23. Burnett, R. et al. Global estimates of mortality associated with long-term exposure to outdoor fine particulate matter. *Proc. Natl Acad. Sci. USA* **115**, 9592–9597 (2018).
24. Lelieveld, J. et al. Effects of fossil fuel and total anthropogenic emission removal on public health and climate. *Proc. Natl Acad. Sci. USA* **116**, 7192–7197 (2019).
25. Driscoll, C. T. et al. US power plant carbon standards and clean air and health co-benefits. *Nat. Clim. Change* **5**, 535–540 (2015).
26. Buonocore, J. J. et al. Health and climate benefits of different energy-efficiency and renewable energy choices. *Nat. Clim. Change* **6**, 100–105 (2016).
27. Prehoda, E. W. & Pearce, J. M. Potential lives saved by replacing coal with solar photovoltaic electricity production in the US. *Renew. Sustain. Energy Rev.* **80**, 710–715 (2017).
28. Millstein, D., Wiser, R., Bolinger, M. & Barbose, G. The climate and air-quality benefits of wind and solar power in the United States. *Nat. Energy* **2**, 17134 (2017).
29. Abel, D. W. et al. Air-quality-related health impacts from climate change and from adaptation of cooling demand for buildings in the eastern United States: an interdisciplinary modeling study. *PLoS Med.* **15**, e1002599 (2018).
30. Abel, D. W. et al. Air quality-related health benefits of energy efficiency in the United States. *Environ. Sci. Technol.* **53**, 3987–3998 (2019).
31. Currie, J., Davis, L., Greenstone, M. & Walker, R. Environmental health risks and housing values: evidence from 1,600 toxic plant openings and closings. *Am. Econ. Rev.* **105**, 678–709 (2015).
32. Luechinger, S. Air pollution and infant mortality: a natural experiment from power plant desulfurization. *J. Health Econ.* **37**, 219–231 (2014).
33. Yang, M. & Chou, S.-Y. The impact of environmental regulation on fetal health: evidence from the shutdown of a coal-fired power plant located upwind of New Jersey. *J. Environ. Econ. Manage.* **90**, 269–293 (2018).

34. Severnini, E. Impacts of nuclear plant shutdown on coal-fired power generation and infant health in the Tennessee valley in the 1980s. *Nat. Energy* **2**, 17051 (2017).
35. Casey, J. A. et al. Increase in fertility following coal and oil power plant retirements in California. *Environ. Health* **17**, 44 (2018).
36. Casey, J. A. et al. Retirements of coal and oil power plants in California: association with reduced preterm birth among populations nearby. *Am. J. Epidemiol.* **187**, 1586–1594 (2018).
37. *QuickStats database* (USDA, accessed 30 January 2018); https://www.nass.usda.gov/Quick_Stats/
38. Myhre, G. et al. in *Climate Change 2013: The Physical Science Basis* (eds Stocker, T. F. et al.) Ch. 8 (IPCC, Cambridge Univ. Press, 2013).
39. Haywood, J. & Shine, K. The effect of anthropogenic sulfate and soot aerosol on the clear sky planetary radiation budget. *Geophys. Res. Lett.* **22**, 603–606 (1995).
40. Charlson, R. J. et al. Climate forcing by anthropogenic aerosols. *Science* **255**, 423–430 (1992).
41. Chylek, P. & Wong, J. Effect of absorbing aerosols on global radiation budget. *Geophys. Res. Lett.* **22**, 929–931 (1995).
42. Chay, K. Y. & Greenstone, M. The impact of air pollution on infant mortality: evidence from geographic variation in pollution shocks induced by a recession. *Q. J. Econ.* **118**, 1121–1167 (2003).
43. Eftim, S. E., Samet, J. M., Janes, H., McDermott, A. & Dominici, F. Fine particulate matter and mortality: a comparison of the six cities and American cancer society cohorts with a medicare cohort. *Epidemiology* **19**, 209–216 (2008).
44. Zeger, S. L., Dominici, F., McDermott, A. & Samet, J. M. Mortality in the medicare population and chronic exposure to fine particulate air pollution in urban centers (2000-2005). *Environ. Health Perspect.* **116**, 1614–1619 (2008).
45. Knittel, C. R., Miller, D. L. & Sanders, N. J. Caution, drivers! children present: traffic, pollution, and infant health. *Rev. Econ. Stat.* **98**, 350–366 (2016).
46. Bell, M. L., McDermott, A., Zeger, S. L., Samet, J. M. & Dominici, F. Ozone and short-term mortality in 95 US urban communities, 1987-2000. *JAMA* **292**, 2372–2378 (2004).
47. Burney, J. & Ramanathan, V. Recent climate and air pollution impacts on Indian agriculture. *Proc. Natl Acad. Sci. USA* **111**, 16319–16324 (2014).
48. Metaxoglou, K. & Smith, A. Productivity spillovers from pollution reduction: reducing coal use increases crop yields. *Am. J. Agric. Econ.* https://doi.org/10.1093/ajae/aaz044 (2019).
49. Brauer, M. et al. Ambient air pollution exposure estimation for the global burden of disease 2013. *Environ. Sci. Technol.* **50**, 79–88 (2015).
50. Apte, J. S., Marshall, J. D., Cohen, A. J. & Brauer, M. Addressing global mortality from ambient $PM_{2.5}$. *Environ. Sci. Technol.* **49**, 8057–8066 (2015).
51. Vodonos, A., Awad, Y. A. & Schwartz, J. The concentration-response between long-term $PM_{2.5}$ exposure and mortality; a meta-regression approach. *Environ. Res.* **166**, 677–689 (2018).
52. Auffhammer, M., Ramanathan, V. & Vincent, J. R. Integrated model shows that atmospheric brown clouds and greenhouse gases have reduced rice harvests in India. *Proc. Natl Acad. Sci. USA* **103**, 19668–19672 (2006).
53. Rollins, A. W. et al. Evidence for NO_x control over nighttime SOA formation. *Science* **337**, 1210–1212 (2012).
54. Zheng, B. et al. Heterogeneous chemistry: a mechanism missing in current models to explain secondary inorganic aerosol formation during the January 2013 haze episode in north China. *Atmos. Chem. Phys.* **15**, 2031–2049 (2015).
55. Levy, J. I., Diez, D., Dou, Y., Barr, C. D. & Dominici, F. A meta-analysis and multisite time-series analysis of the differential toxicity of major fine particulate matter constituents. *Am. J. Epidemiol.* **175**, 1091–1099 (2012).
56. Thurston, G. D. et al. Ischemic heart disease mortality and long-term exposure to source-related components of US fine particle air pollution. *Environ. Health Perspect.* **124**, 785–794 (2015).
57. Bell, M. L. & Ebisu, K. Environmental inequality in exposures to airborne particulate matter components in the United States. *Environ. Health Perspect.* **120**, 1699–1704 (2012).
58. Hsu, A., Reuben, A., Shindell, D., de Sherbinin, A. & Levy, M. Toward the next generation of air quality monitoring indicators. *Atmos. Environ.* **80**, 561–570 (2013).
59. Ryerson, T. et al. Observations of ozone formation in power plant plumes and implications for ozone control strategies. *Science* **292**, 719–723 (2001).
60. Shindell, D. & Faluvegi, G. The net climate impact of coal-fired power plant emissions. *Atmos. Chem. Phys.* **10**, 3247–3260 (2010).
61. Burnham, A. et al. Life-cycle greenhouse gas emissions of shale gas, natural gas, coal, and petroleum. *Environ. Sci. Technol.* **46**, 619–627 (2011).
62. Berntsen, T., Fuglestvedt, J., Myhre, G., Stordal, F. & Berglen, T. F. Abatement of greenhouse gases: does location matter? *Climatic Change* **74**, 377–411 (2006).
63. Shindell, D. T. The social cost of atmospheric release. *Climatic Change* **130**, 313–326 (2015).
64. Aakre, S., Kallbekken, S., Van Dingenen, R. & Victor, D. G. Incentives for small clubs of arctic countries to limit black carbon and methane emissions. *Nat. Clim. Change* **8**, 85–90 (2018).
65. van Donkelaar, A. et al. Global estimates of fine particulate matter using a combined geophysical-statistical method with information from satellites, models, and monitors. *Environ. Sci. Technol.* **50**, 3762–3772 (2016).
66. *Air Quality Reports Input Data* (EPA, accessed 9 September 2019); https://www.epa.gov/hesc/rsig-related-downloadable-data-files
67. Bhartia, P. K. *OMI/Aura Ozone (O3) Total Column Daily L2 Global Gridded 0.25 degree x 0.25 degree V3* (Goddard Earth Sciences Data and Information Services Center, 2012); https://doi.org/10.5067/Aura/OMI/DATA2025
68. Krotkov, N. A., Li, C. & Leonard, P. *OOMI/Aura Sulphur Dioxide (SO2) Total Column Daily L2 Global Gridded 0.125 degree x 0.125 degree V3* (Goddard Earth Sciences Data and Information Services Center, 2014); https://doi.org/10.5067/Aura/OMI/DATA2023
69. Boersma, K. F. et al. An improved retrieval of tropospheric NO_2 columns from the Ozone Monitoring Instrument. *Atmos. Meas. Tech.* **4**, 1905–1928 (2011).
70. Torres, O. O. *OMAERUVd: OMI/Aura Near UV Aerosol Optical Depth and Single Scattering Albedo L3 1 day 1.0 degree x 1.0 degree V3* (NASA Goddard Space Flight Center, Goddard Earth Sciences Data and Information Services Center, 2008); https://doi.org/10.5067/Aura/OMI/DATA3003
71. Platnick, S. et al. *MODIS Atmosphere L3 Monthly Product* (NASA MODIS Adaptive Processing System, Goddard Space Flight Center, 2015); https://doi.org/10.5067/MODIS/MOD08_M3.006
72. AIRS Science Team/Teixeira, J. *AIRS/Aqua L3 Monthly Standard Physical Retrieval (AIRS-only) 1 degree x 1 degree V006* (Goddard Earth Sciences Data and Information Services Center, 2013); https://doi.org/10.5067/Aqua/AIRS/DATA321
73. *M2TMNXRAD: MERRA-2 tavgM_2d_rad_Nx: 2d,Monthly mean,Time-Averaged,Single-Level,Assimilation,Radiation Diagnostics V5.12.4* (GMAO, 2015); https://doi.org/10.5067/OU3HJDS973O0
74. *Compressed Mortality File* (US Centers for Disease Control (CDC) National Vital Statistics Service 2005–2016, accessed 1 February 2018); https://wonder.cdc.gov/controller/datarequest/D140
75. Coakley, G. & Chylek, P. The two-stream approximation in radiative transfer: including the angle of the incident radiation. *J. Atmos. Sci.* **32**, 409–418 (1975).
76. Russell, P., Kinne, S. & Bergstrom, R. Aerosol climate effects: local radiative forcing and column closure experiments. *J. Geophys. Res. Atmos.* **102**, 9397–9407 (1997).
77. Delene, D. J. & Ogren, J. A. Variability of aerosol optical properties at four North American surface monitoring sites. *J. Atmos. Sci.* **59**, 1135–1150 (2002).

Acknowledgements

I thank the Policy Design and Evaluation Lab and Big Pixel Initiative (both at UC San Diego), and the National Science Foundation (CNH Award no. 1715557) for funding.

Competing interests

The author declares no competing interests.

Additional information

Extended data is available for this paper at https://doi.org/10.1038/s41893-019-0453-5.

Supplementary information is available for this paper at https://doi.org/10.1038/s41893-019-0453-5.

Correspondence and requests for materials should be addressed to J.A.B.

Reprints and permissions information is available at www.nature.com/reprints.

Publisher's note Springer Nature remains neutral with regard to jurisdictional claims in published maps and institutional affiliations.

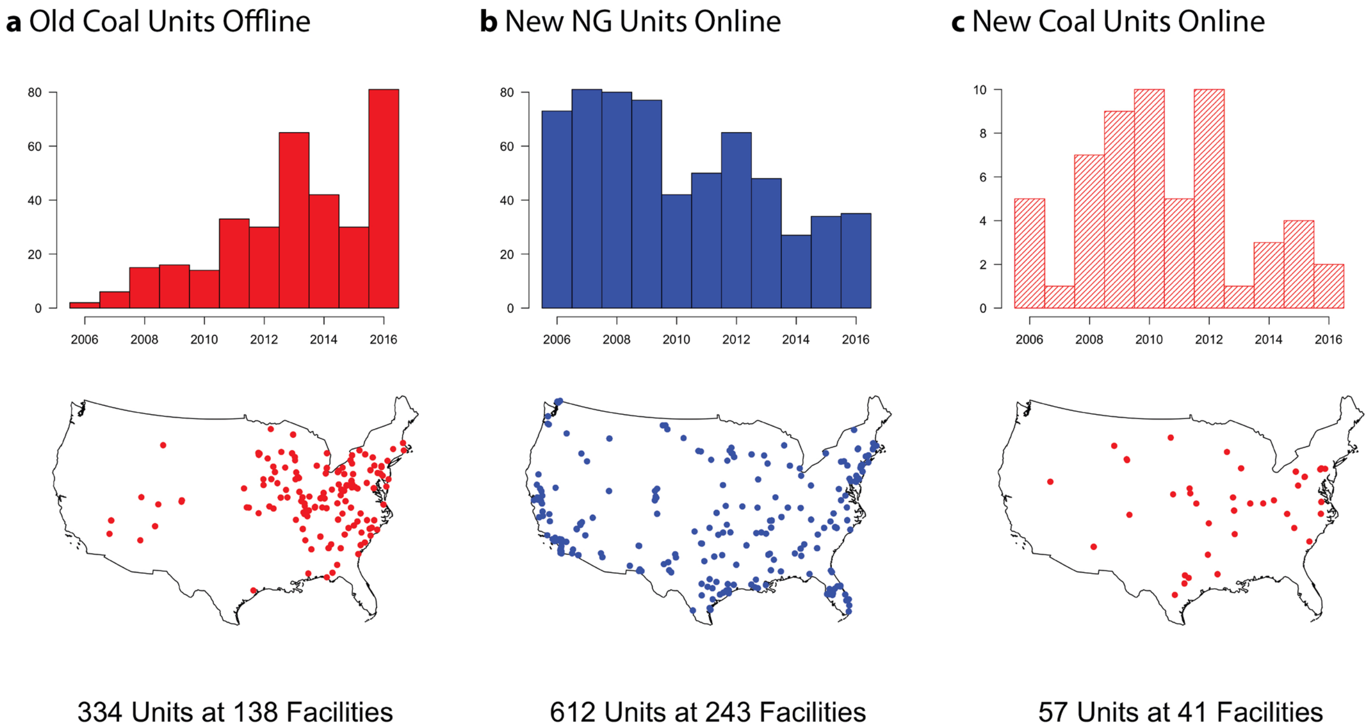

Extended Data Fig. 1 | Temporal and geographic distribution of old coal units taken offline, new natural gas units brought online, and new coal units brought online in the United States, 2005-2016. These technological changes (closing and opening of new and old electric power generation units) occur at discrete moments in time, resulting in changes in emissions fluxes into the surrounding area. These changes are assumed to be as-if random in space and time, vis-à-vis each other, and discontinuities in ambient conditions are estimated across the sample for these natural experiments (see Methods).

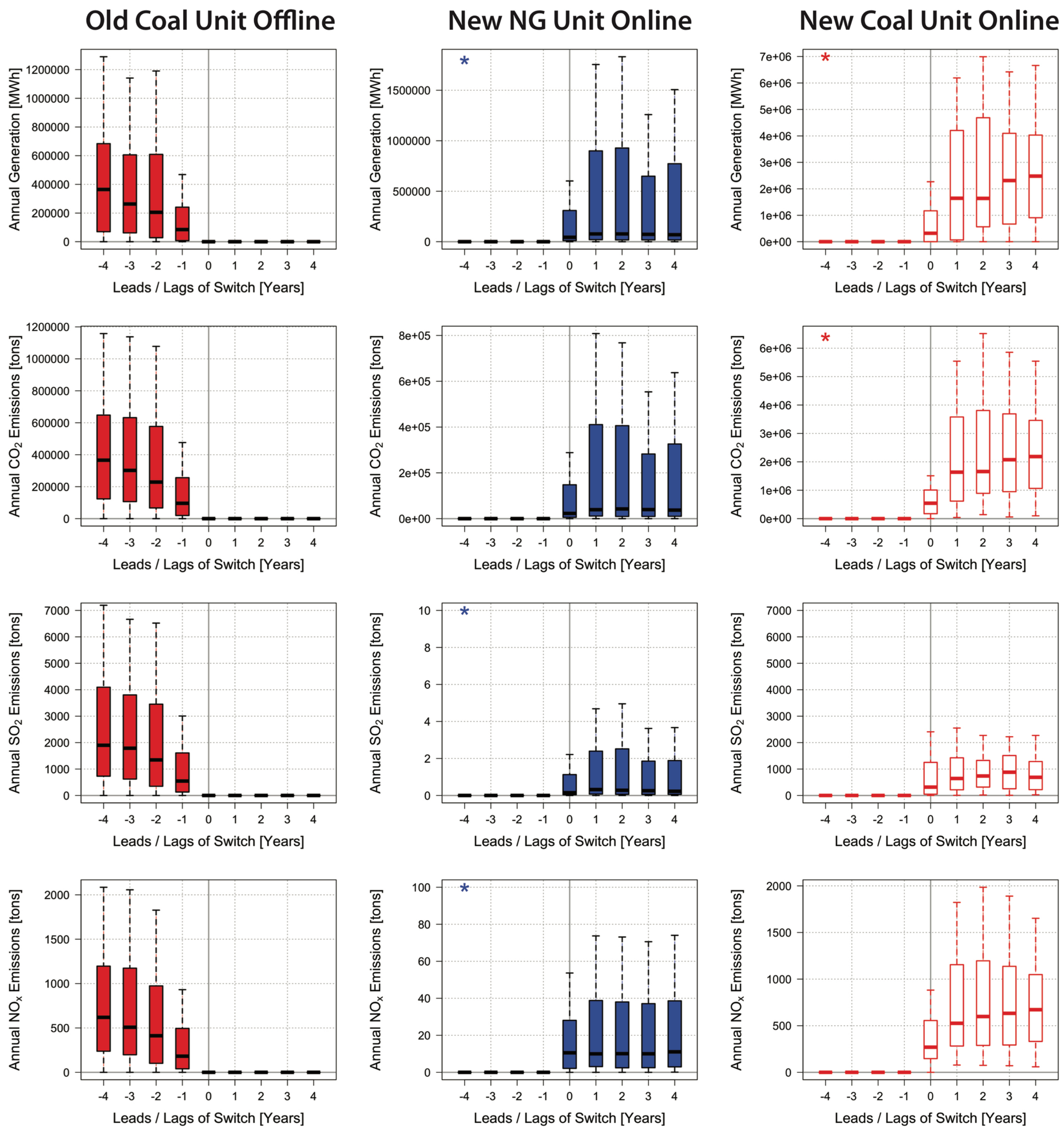

Extended Data Fig. 2 | Emissions of CO_2, SO_2, and NO_x associated with shutdown of old coal-fired units, and start-up of new natural gas-fired and coal-fired units. (Left Column) Coal-fired units approaching decommissioning are often 'ramped down' prior to shutdown, as reflected in decreasing gross load and emissions. (Centre and Right Columns) Conversely, as they ramp up after commissioning, new units may take some time to settle into steady-state. Further downstream impacts of a coal unit shut-down are thus likely to begin to manifest in the year prior to final closure, and impacts of new units may change over time. Boxes show the 25th-75th percentiles, with the median indicated by the bar, with whiskers indicating the 2.5 to 97.5 percentile confidence interval; values outside of this range are not shown. (Note the different scales for new coal unit generation and CO_2 emissions, and for new natural gas generation and NO_x and SO_2 emissions, marked with asterisks).

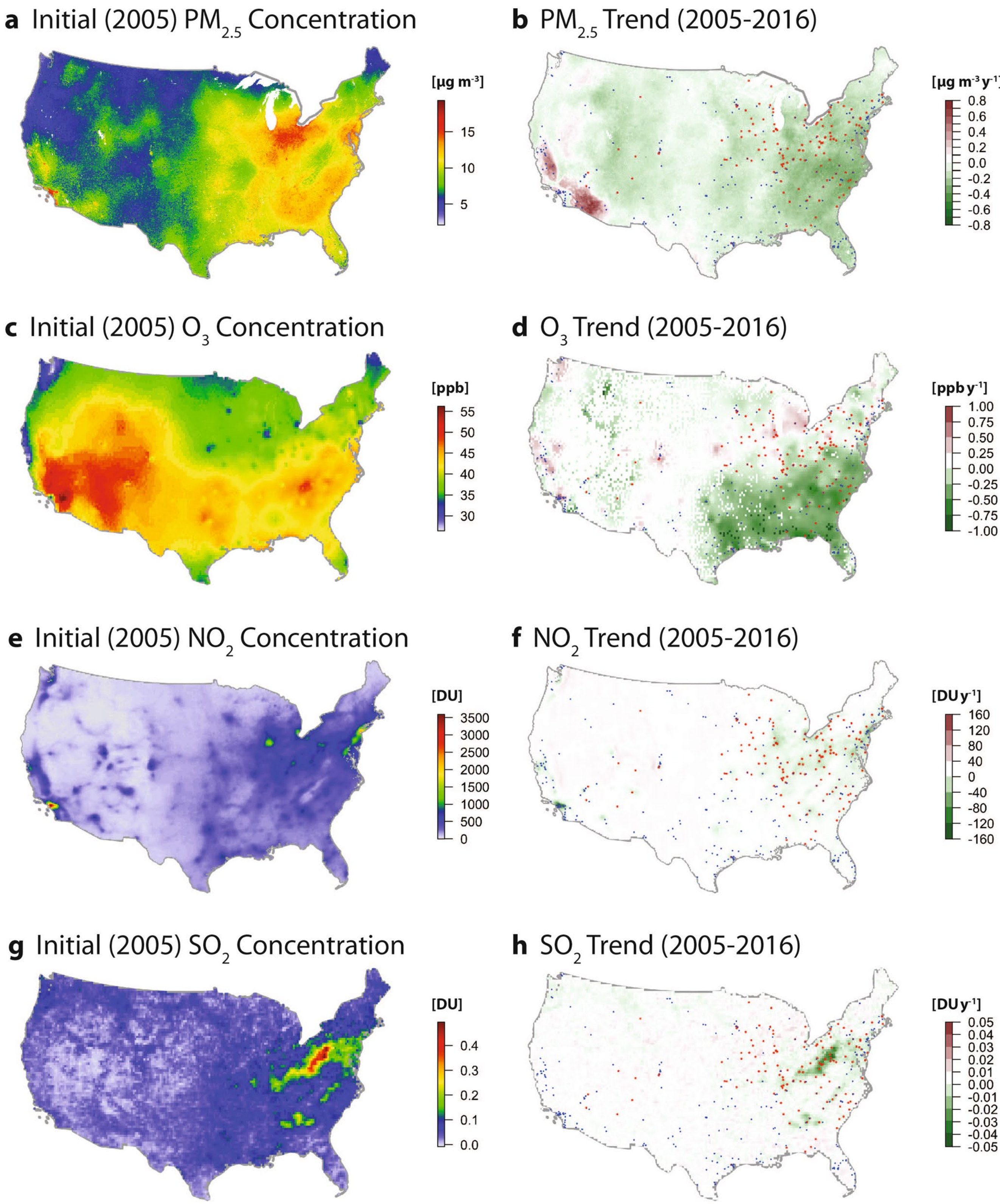

Extended Data Fig. 3 | Starting (2005) levels and trends over the study period for $PM_{2.5}$, O_3, SO_2, and NO_2. Dots in the trends plots show locations of coal-fired units taken offline (red) and natural gas-fired units brought online (blue) during the study period. As shown in this analysis, part of these changes is attributable to shifts in electric power production feedstock, but other policies and regulations (for example fuel efficiency standards) and technology changes (for example emissions controls technologies) have contributed as well. Coal and diesel combustion are responsible for most SO_2 emissions, while NO_2 (a portion of NO_x) comes from transportation as well as combustion of coal and natural gas. NO_2 concentrations are more tightly associated with urban areas and transportation corridors. Ozone production is nonlinear, based on reactions of NO_x and volatile organic compounds in the presence of sunlight. Particulate Matter includes aerosols from many sources, including primary carbonaceous aerosols, sulfates (from SO_2), nitrates (in part from NO_x), dust, and sea salt (see Supplementary Fig. 1).

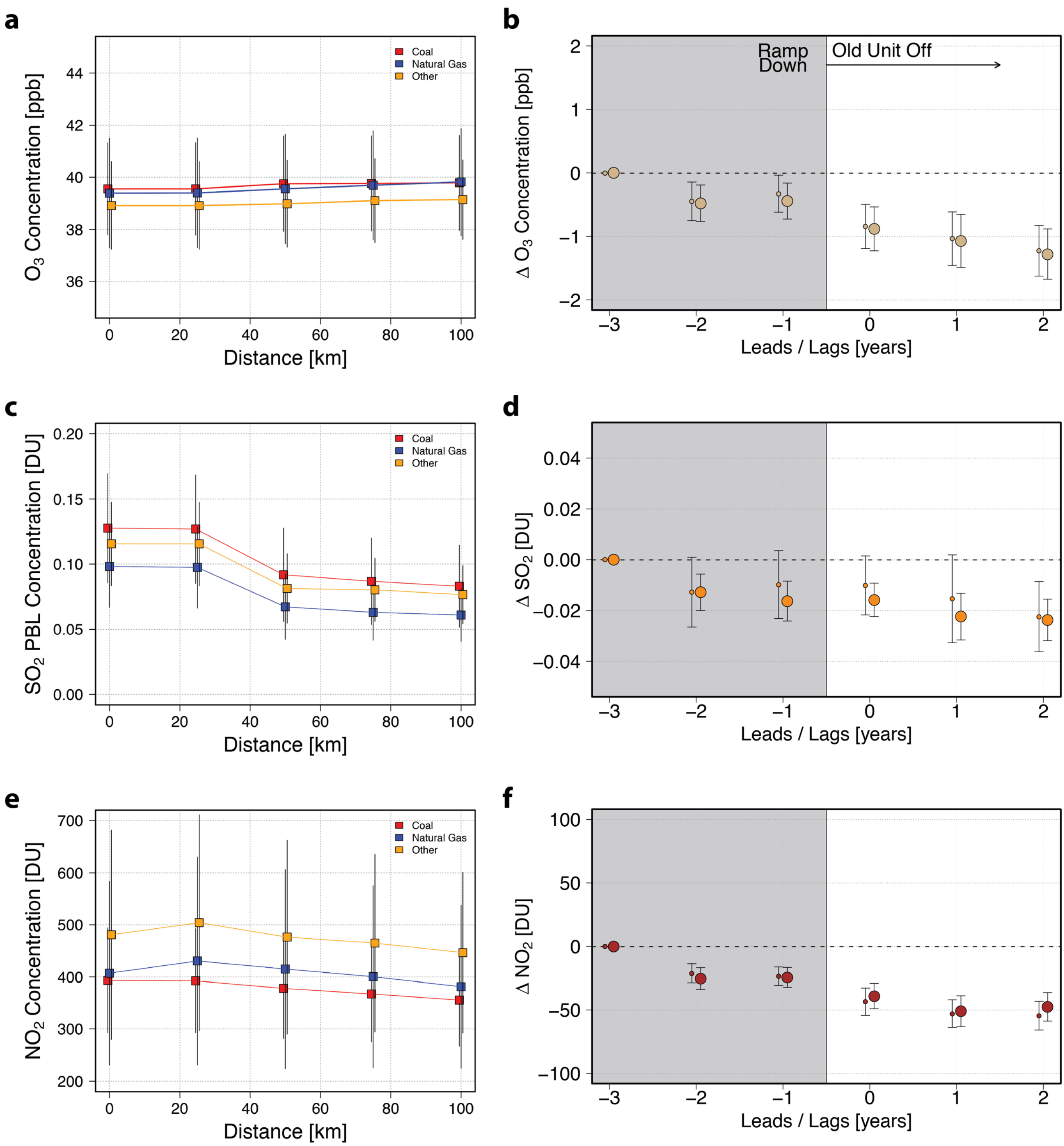

Extended Data Fig. 4 | Pollution surrounding power plant locations. (**a**,**c**,**e**) As in Fig. 2b: Average surface O_3, near-surface (Planetary boundary Layer) SO_2, and tropospheric NO_2 surrounding operating electric power plants, by fuel type. SO_2 and NO_2 decrease radially around plants. Although SO_2 is not a main byproduct of natural gas combustion, some plants have a combination of gas and coal-fired units, and others may use different types of fuels. Ozone dynamics are more complicated around an emissions source, consistent with previous studies. (**b**,**d**,**f**) As in Fig. 2a: Raw average changes in ambient O_3, SO_2, and NO_2 in the time leading up to, and after, a coal-fired unit shutdown. Estimates include location-level fixed effects (that is concentrations for each location are de-meaned to show changes from baseline). Error bars show the 5th-95th% confidence interval, based on standard errors clustered at the location level.

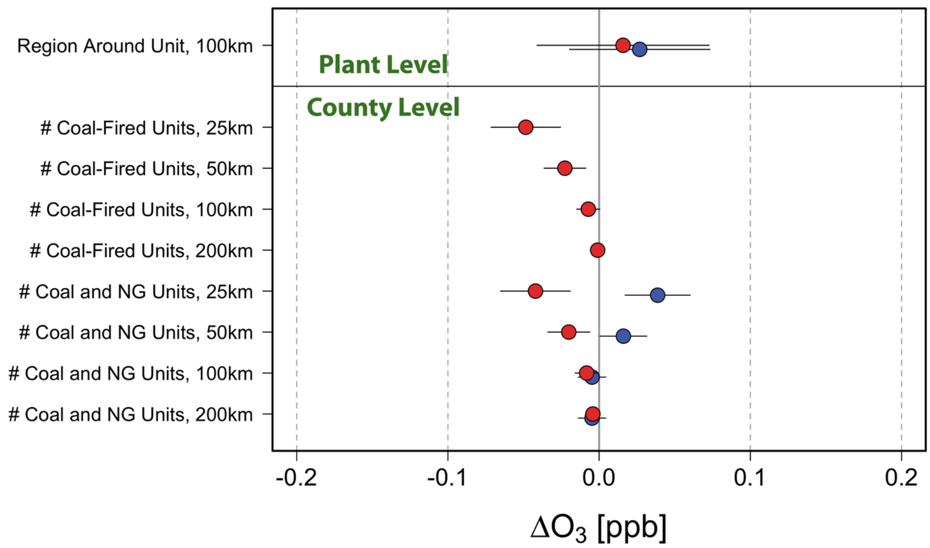

Extended Data Fig. 5 | Comparison of surface ozone impacts of power generation units. As in Fig. 2c. Comparison of different models relating a change in number of units of a given feedstock within a given radius of a county, and average levels of O_3 in that county. Addition of a natural gas-fired unit is associated with increased ozone levels (likely via increased NO_x production).

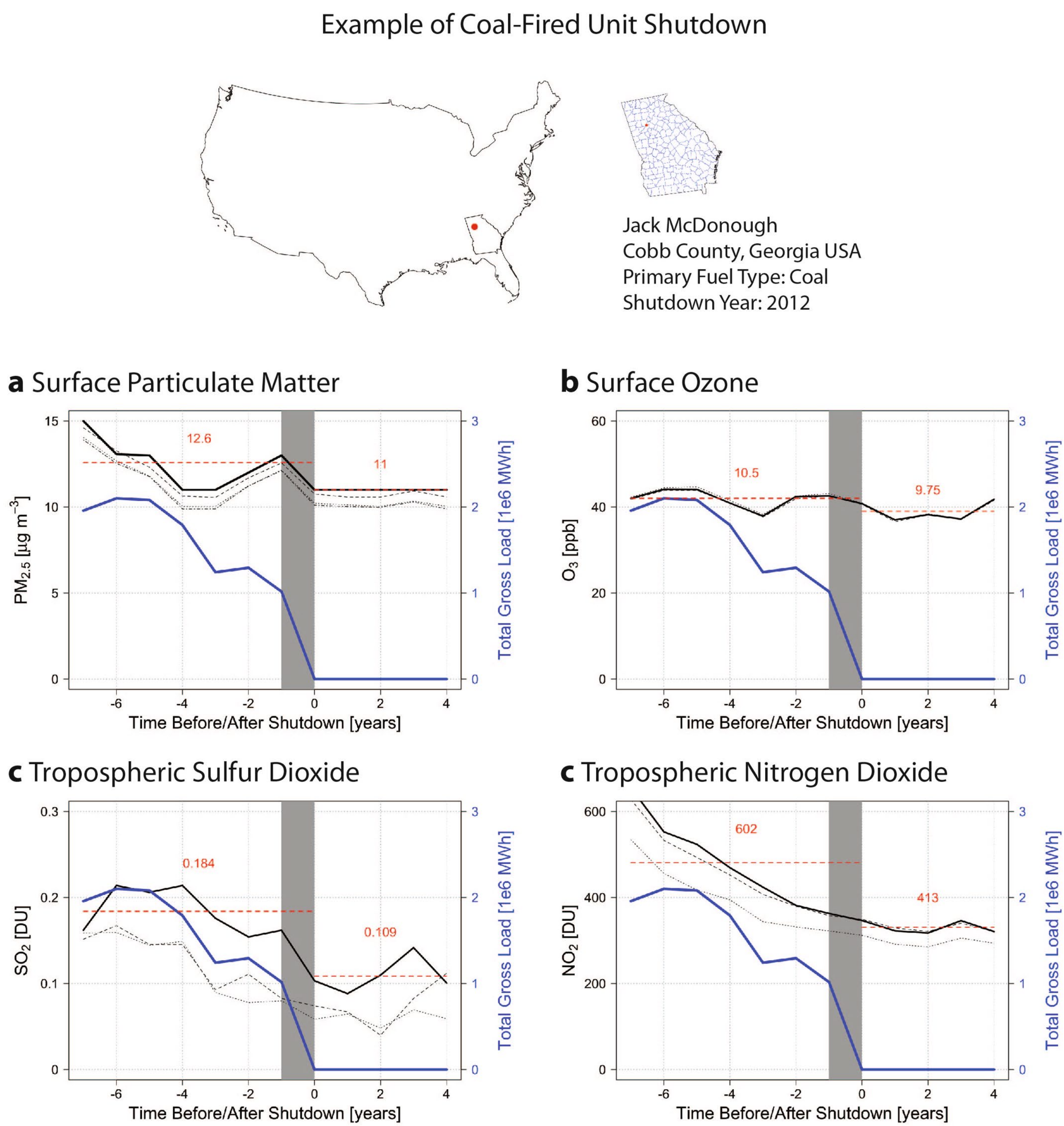

Extended Data Fig. 6 | One example location. Data from a coal-fired unit shut down in Georgia, showing the changes in ambient $PM_{2.5}$, O_3, SO_2, and NO_2. The thick blue line shows power generation (gross load), with the shutdown marked by the grey bar. Black lines show pollutant concentrations: the solid line shows concentration of each pollutant in the immediate region around the power plant, with dashed lines out to a 100km radius. This is an individual instance of the aggregate averages presented in the main text (Fig. 2, as well as Figures ED2 and ED5, and all Supplementary Tables).

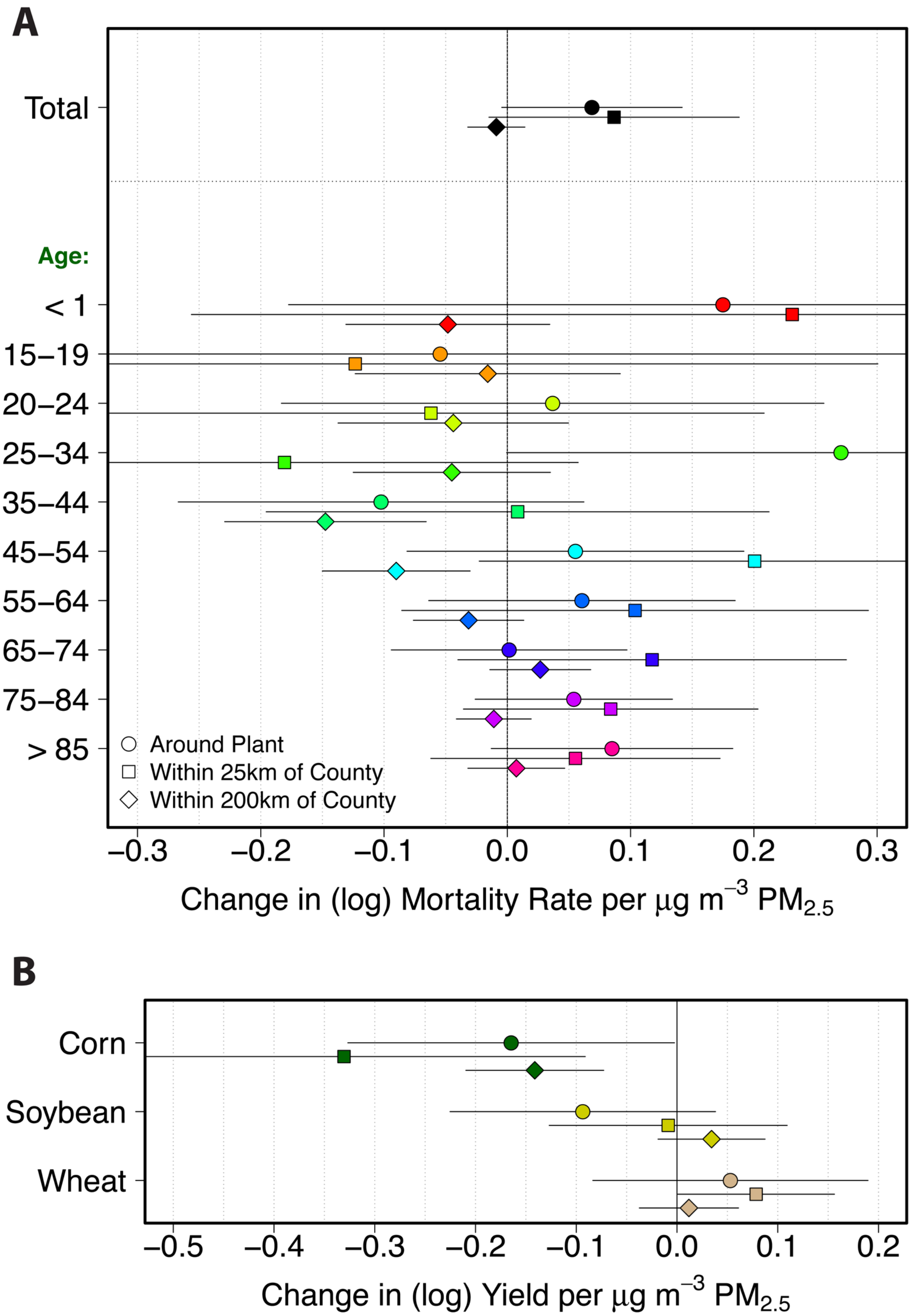

Extended Data Fig. 7 | Instrumental variables impact estimates. As in Fig. 3a,b, only using an instrumental variables approach to estimate the effect of a 1 µg m^{-3} increase in $PM_{2.5}$ on mortality and crop yields. In this approach, coal unit shutdowns are first related to $PM_{2.5}$ concentrations; those predicted $PM_{2.5}$ values are then related to mortality and crop yields. This approach strips out the variation in aerosol $PM_{2.5}$ and other covarying pollutants not associated with unit shutdown. Central estimates are similar to Fig. 3a,b (but with larger error bars) indicating robustness of the approach of relating unit shutdowns directly to downstream outcomes. However, results should be interpreted as the impact of all pollutants covarying with $PM_{2.5}$, and not $PM_{2.5}$ alone.

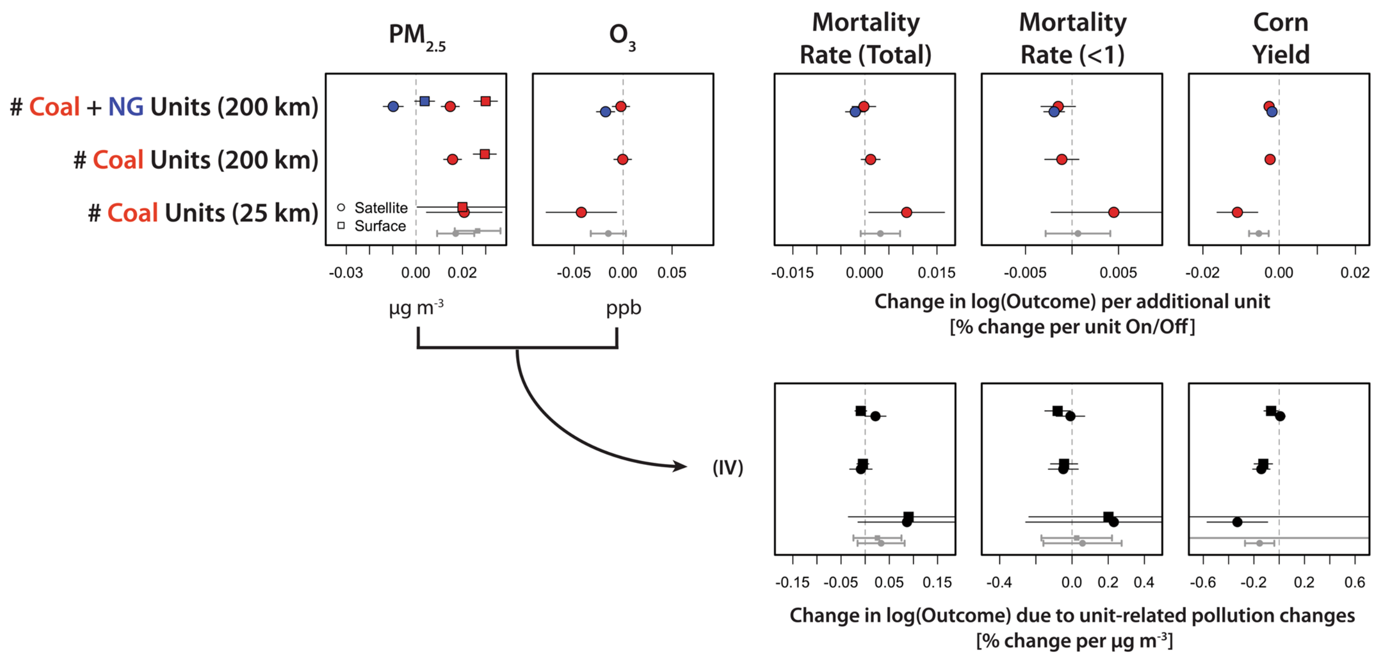

Extended Data Fig. 8 | A summary of impacts results estimated from different models at the county level. The top row shows reduced form results for pollution, mortality, and crop impacts for 3 county-based models. The 25km and 200km coal models are shown in Fig. 2 and Fig. 3 in the main text. The third (top set of points) model includes natural-gas fired units. Red dots indicate coal unit impacts, and blue dots indicate natural gas unit impacts. The bottom row shows a comparison of instrumental variables (IV) results, whereby the number of units within a given radius is first related to changes in ambient pollution; those changes in pollution are then related in a second step to outcomes. Although results are cast as per µg m^{-3}, they should be interpreted as the impacts of all pollution that covaries with $PM_{2.5}$. The robustness of these IV results across models highlights the need for more causally-identified impacts studies and provides evidence that natural gas-fired units are not benign. error bars show the 5th-95th percentile confidence interval; all estimates include county and year fixed effects, with standard errors clustered at the county level. Small grey bars show the average of the three models for each outcome. Surface $PM_{2.5}$ estimates for corn are large and unstable (Supplementary Tables 7–9).

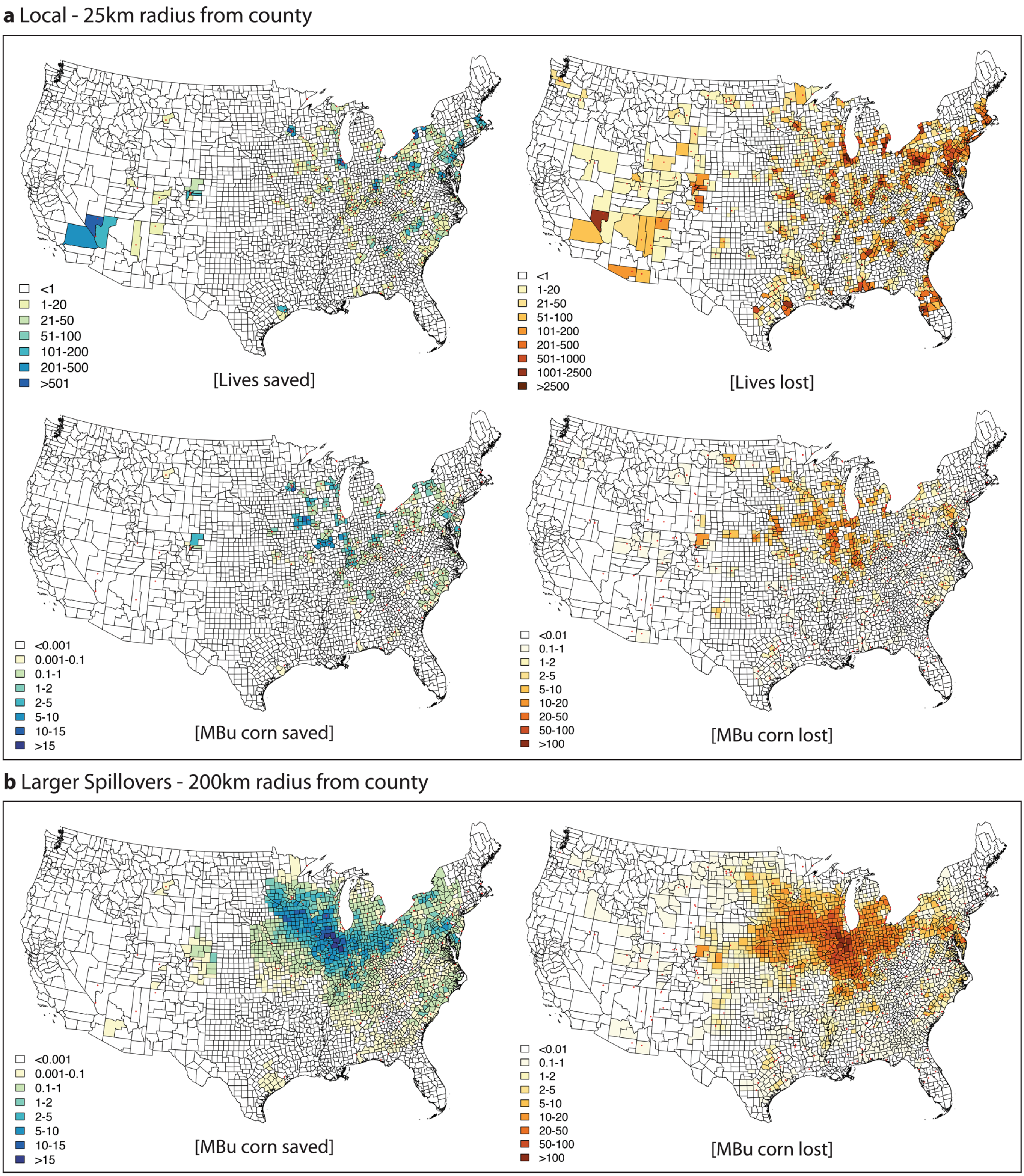

Extended Data Fig. 9 | Total impacts of coal-fired fleet. a, The left two panels are the same as Fig. 3c–d, showing mortality and crop yield impacts integrated over the study period for plants within 25km from each county. The right column shows the calculation described for impacts of remaining coal-fired units still operating, assuming that their impacts are the same as those that have been decommissioned. **b**, Corn yield impacts integrated over the study period for plants within 200km from each county. As in **a**, the left panel shows the impacts of units shut down, and the right panel shows the estimated impacts of coal-fired units that remained in operation.

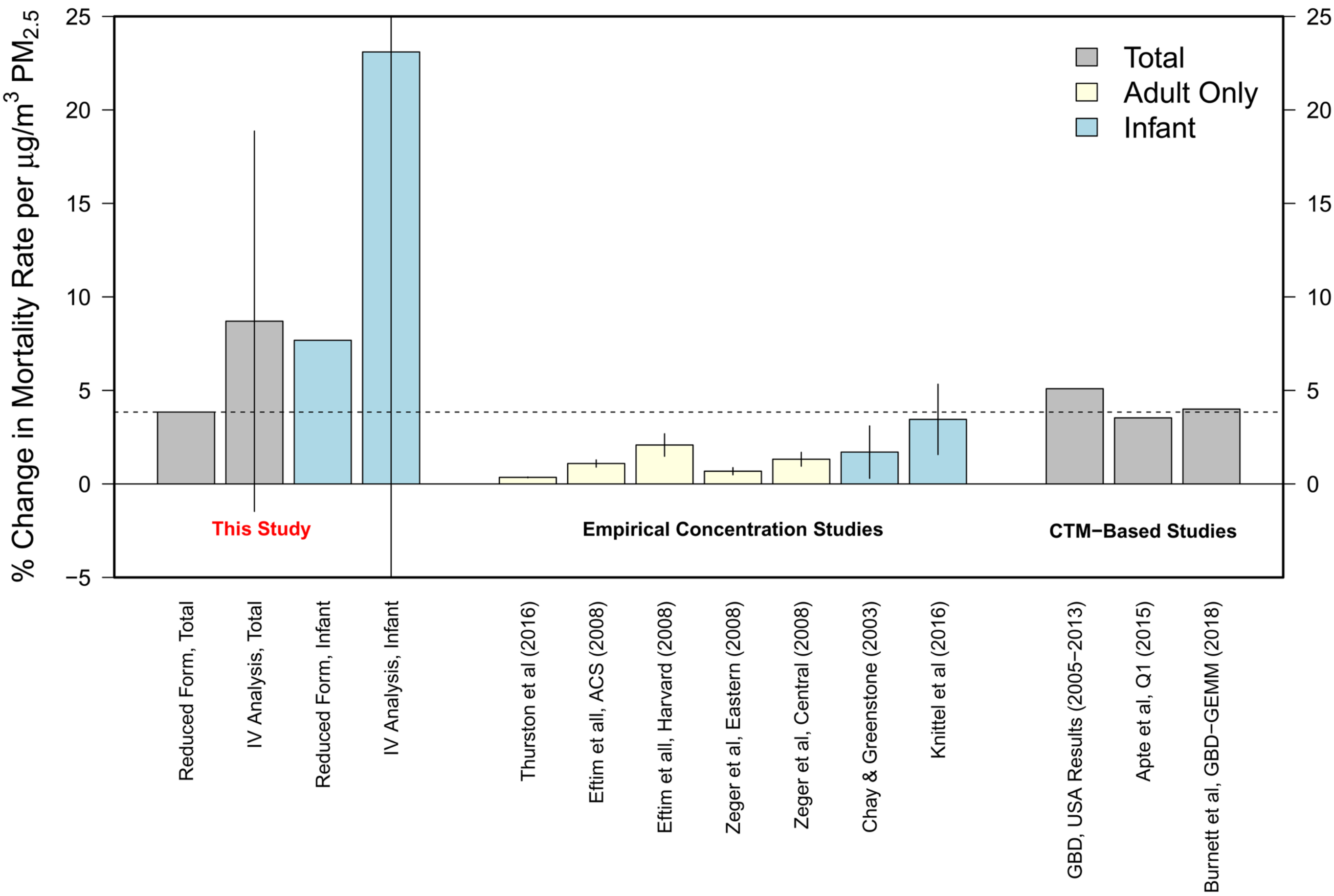

Extended Data Fig. 10 | Comparison between mortality results from this study and other literature. Central reduced-form mortality estimates in this study, converted to a per-µg m^{-3} basis, are similar to previous empirical exposure studies, for both total mortality and infant mortality. The Thurston et al, Eftim et al, and Zeger et al studies all focused on adults; Chay & Greenstone and Knitell et al focus on infant mortality. GBD results (2005-2013) are derived by combining $PM_{2.5}$ reduction estimates from and pollution mortality from the GBD web interface. Apte et al results are for the lowest quartile (U.S. in that category), cast as percentages, and Burnett et al are estimated from the GEMM total mortality curve provided in the paper. Although not statistically significant (error bars show 5th-95th percentile confidence interval) the instrumental variables estimates from this analysis nevertheless highlight the importance of future causally-identified observational studies, as well as the critical role more comprehensive monitoring may play in reducing measurement errors (see Figure ED8).